Journal of King Saud University – Computer and Information Sciences 31 (2019) 469–480

Contents lists available at ScienceDirect

Journal of King Saud University – Computer and Information Sciences

journal homepage: www.sciencedirect.com

Proposed optimized hybrid error recovery techniques for performance improvement of wireless 3D-MVC communication

W. El-Shafai *, S. El-Rabaie, M. El-Halawany, F.E. Abd El-Samie

Department of Electronics and Electrical Communications Engineering, Faculty of Electronic Engineering, Menoufia University, 32952 Menouf, Egypt

ARTICLE INFO

Article history:
Received 1 November 2017
Revised 14 January 2018
Accepted 18 February 2018
Available online 26 February 2018

Keywords:
Packet loss concealment
3D multi-view video
Motion and disparity compensation
Depth maps
Spatio-temporal-inter-view correlations
Wireless channels

ABSTRACT

The transmission of 3D Video (3DV) over wireless channels has become a hot issue because of the limited resources and the existence of severe channel errors. In the 3DV system, the compressed bit streams may be dropped down due to the propagation of transmission errors in the time, space, and view scopes. So, it is important to recover the Disparity Vectors (DVs) and Motion Vectors (MVs) of the corrupted Macro-Blocks (MBs) at the decoder utilizing efficient Error Concealment (EC) post-processing techniques. To enhance the received 3DV quality, we suggest optimized hybrid techniques to reconstruct the erroneous MBs of color-plus-depth inter-encoded and intra-encoded frames. A hybrid approach of Circular Scan Order Interpolation (CSOI) technique and Partitioning Motion Compensation (PMC) technique is proposed for the color intra-frames loss concealment. For the corrupted color inter-frames, a joint approach of Directional Textural Motion Coherence (DTMC) technique and Directional Interpolation Error Concealment (DIEC) technique is suggested. To estimate more additional depth-aided DVs and MVs for recovering the erroneous depth frames, a depth-assisted error recovery technique is suggested. These depth-estimated motion and disparity vectors are then added together with the estimated candidate texture DVs and MVs for reconstructing the corrupted color-plus-depth frames. Finally, the best color-plus-depth MVs and DVs are chosen by the Decoder Motion Vector Estimation (DMVE) and DIEC techniques. Simulation outcomes on various 3D video frames elucidate that the suggested hybrid color plus depth EC techniques achieve high robustness at high Packet Loss Rates (PLRs).

1. Introduction

The standard of Multi-view Video Compression (MVC) (Xiang et al., 2015; Ozcinar et al., 2016; Purica et al., 2016) achieves efficient 3D video encoding. This standard is a complement of the 2D video compression standard (H.264/AVC, 2016), and it is predicted to quickly take place of the 2D H.264 in various implementations. In the 3D-MVC system, the 3DV comprises diverse sequences picked for the selfsame object with different cameras. Thence, it is an insistent mission to attain sufficient compression to fulfill future bandwidth requirements, whilst preserving a decisive 3DV reception quality. To transmit 3DV over limited-resources channels, a highly sufficient encoding process must be utilized, whilst maintaining an appreciated reception quality (De Abreu et al., 2015). For efficient 3DV communication, the 3D-MVC system must benefit from the spatial and temporal matching among neighboring frames in the selfsame video besides the inter-view correlation inside various 3D video sequences to improve the compression efficiency. However, video compression with high rates is more susceptible to transmission channel corruptions.

The 3DV transmission through wireless channels is permanently subject to packet errors of both burst and random natures (El Shafai, 2011; Hewage and Martini, 2013; Liu et al., 2013). The predictive 3D MVC Prediction Structure (MVC-PS) introduced in Fig. 1 (El-Shafai, 2015; El-Shafai, 2015) is used to compress the 3DV streams. It utilizes the Motion Compensation Prediction (MCP) and Disparity Compensation Prediction (DCP) at the encoder side to achieve efficient 3DV encoding, and at the decoder side, it executes an efficient error concealment process. In the MVC-PS presented in Fig. 1, the vertical axis refers to time, whereas the horizontal line refers to the different views of the cameras. So, the V notation refers to the captured view index. The even views (V2, V4, and V6) are compressed depending on the motion

* Corresponding author.
E-mail address: eng.waled.elshafai@gmail.com (W. El-Shafai).

Peer review under responsibility of King Saud University.

Production and hosting by Elsevier

https://doi.org/10.1016/j.jksuci.2018.02.007
1319-1578/

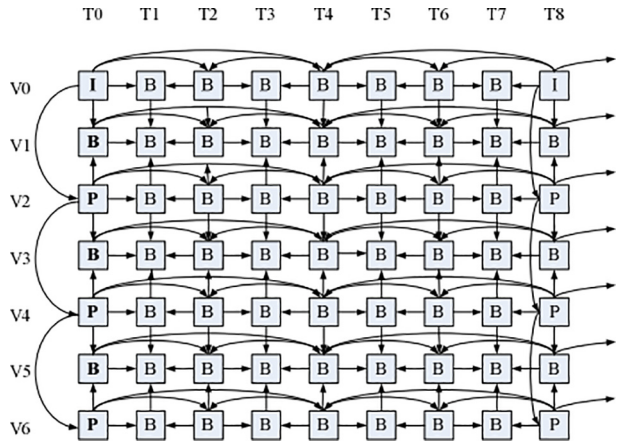

Fig. 1. 3D video compression prediction structure.

compensation, while their prime key frames are compressed through the use of disparity compensation. The V0 view is compressed using only time matching based on the MCP. On the other hand, in the odd views (V1, V3 and V5), the MCP and DCP are jointly utilized for improving the compression efficiency. The even views are named as the P views, the V0 view is called the I view, and the odd views are called the B views.

The 3DV MVC prediction structure in Fig. 1 presents a Group-of-Pictures (GoPs) that comprises two different types of compressed frames, which are the I intra-frames and the B and P frames. The B views inter-frames are determined using the I view intra-frames and also from the P views inter-frames. Thence, if an error occurs at the P or I frame, it propagates to the reference inter-view frames, and moreover to the neighboring time pictures in the self-same 3DV view, and thus it creates destitute 3DV quality. To minimize the effect of packet losses before 3DV transmission, in the literature works, the Automatic Repeat Request (ARQ) and Forward Error Correction (FEC) methods have been utilized (Salim et al., 2013; Huo et al., 2013). Unfortunately, they introduce more delay, because they increase the transmission bit rate. Therefore, there is an exigency for post-processing concealment techniques at the decoder side (Khattak et al., 2016; Zhou et al., 2015; Lee et al., 2014; El-Shafai, 2013). They take the merit of the intra- and inter-view correlations inside the 3DV sequences to conceal the lost MBs or frames. They are recommended as they decrease the transmission errors without increasing the delay or requiring complicated encoder side modifications. The EC techniques suggested to conceal the 1-D or 2-D videos can be exploited to recover the lost 3DV MBs (Hwang et al., 2008; Lie et al., 2014; Gadgil et al., 2015). They are anticipated to perform more effectively in recovering the losses of the 3DV MBs due to the advantage of exploiting the inter-view matching (El-Shafai, 2015). In this work, we propose various states of concealment presumptions for color-plus-depth intra- and inter- frames in the P, I, and B views. Thus, the suggested hybrid concealment techniques efficiently choose the suitable EC technique based on the erroneous frame view and type to reconstruct the corrupted color-plus-depth MBs.

The 3D Video-plus-Depth (3DV+D) EC research area has received much attention, recently (Khattak et al., 2016; Zhou et al., 2015; Lee et al., 2014). The 3DV+D is a form of 3D video transmission that has expanded widely (Purica et al., 2016; De Abreu et al., 2015; Khattak et al., 2016). It has data about the scene-per-pixel geometry, because all object pixels must have identical depth values. So, we can utilize the depth information to recognize the object boundaries that will assist the EC mechanism. Furthermore, it optimizes the storage space of the 3DV bits compared to the 2D video bits. In the state-of-the-art works, various depth-aided concealment methods have been widely used for the 2D H.264 video compression standard. Recently, the depth-aided EC techniques for 3D video communication have captured the interest of researchers (Yan and Zhou, 2012; El-Shafai et al., 2017a,b; Chung et al., 2011; Lie and Lin, 2013; Tai et al., 2016; Assunçao et al., 2017; Wang and Wang, 2016; Mueller and Vetro, 2014).

It is noticed almost of the literature depth-aided concealment techniques allow the depth data to be encoded and transmitted over the transmission channel to the decoder, and thus they extract them at the encoder. Therefore, they increase the bit rate and the computational complexity of the 3DV communication system, and hence they are not appropriate for the limited resources of the wireless transmission system. In this paper, an improved depth-assisted concealment scheme is proposed to recover the corrupted depth frames within the 3DV-plus-Depth wireless communication system. The proposed depth-assisted EC scheme in this work estimates the depth data of the severe erroneous frames at the decoder side instead of executing derivations and calculations at the encoder side. This is performed by predicting the DVs and MVs of the received color-plus-depth 3DV data. Therefore, the suggested depth-based scheme can introduce more appreciated subjective and objective qualities than those attained with the previous depth-assisted EC methods, while introducing a minimal computational complexity and optimizing the communication bit rate. It neither increases the transmission latency nor needs difficult encoder procedures. The suggested techniques can also work efficiently with the state of severe frame corruptions neglected in the previous works (Yan and Zhou, 2012; El-Shafai et al., 2017a,b; Chung et al., 2011; Lie and Lin, 2013; Tai et al., 2016; Assunçao et al., 2017; Wang and Wang, 2016; Mueller and Vetro, 2014) and can transport the 3DV data efficiently through wireless networks with heavy losses.

The proposed hybrid error recovery methods are exploited to estimate the optimum MVs and DVs for concealing the corrupted MBs and enhancing the reconstructed 3DV quality. The convenient EC scheme is adaptively employed based on the view type and the lost frame. A hybrid approach of the CSOI and PMC techniques is suggested for concealing the color intra-frame errors. For the corrupted color inter-frames, a joint approach of the DTMC and DIEC techniques is employed. For the lost intra- and inter-depth frames, an efficient depth-aided scheme is suggested to reconstruct the lost depth MBs. The rest of this work is coordinated as follows. Section 2 explains the related basic error recovery techniques. In Section 3, we introduce the suggested dynamic error recovery techniques for the erroneous color MBs and the proposed depth-assisted error recovery scheme for the corrupted depth MBs. Section 4 discusses the experimental results and presents a comparative analysis. In Section 5, we give the concluding remarks of the whole work.

2. Basic error recovery techniques

The 3D video communications over erroneous networks may face huge challenges because of the propagation of packet losses or bit errors that crumble the received and decoded 3D video quality. Therefore, it is a beneficial methodology to use the concealment mechanism for efficient 3D video communication. The concealment process is a dynamic solution to recover and exchange the corrupted 3D video frames by formerly recovered and decoded frames of the 3D stream to eliminate or minimize the video faults. The concealment methods used in the 2D video system to deal with transmission corruptions (Hwang et al., 2008; Lie et al., 2014; Gadgil et al., 2015) may be exploited with some adjustments to compensate for the lost 3DV frames. These

concealment methods are predicted to be further beneficial for concealing the transmission faults in the 3D video system, because they benefit from the inter-view matching between various 3D video views. The Frame Temporal Replacement (FTR) technique is a direct temporal concealment method that substitutes the lost frames by the space frames in the reference matched frame. The Outer Block Boundary Matching (OBBM) and DMVE techniques are more sophisticated temporal EC techniques (Hwang et al., 2008).

The OBBM technique determines the MVs amidst the outer boundaries of the replaced MB pixels and the selfsame external boundaries of the lost MB pixels. It uses only the relative MB outer outlines to put the highest matched neighboring MVs as shown in Fig. 2a. The DMVE technique estimates the erroneous MVs of the frames by applying a perfect search in their reference 3D video frames. It is useful in specifying the interchange of frames that minimizes the loss distortion boundary as shown in Fig. 2b. The DMVE technique introduces a more efficient concealment performance than that of the OBBM technique with nearly the selfsame complexity. The Weight-Pixel-Averaging Interpolation (WPAI) and DIEC techniques are applied for the spatial and inter-view concealment process (Gadgil et al., 2015). The WPAI technique recovers the corrupted MB data by utilizing the vertical and horizontal MB data in the neighboring MBs as shown in Fig. 2c. In the WPAI technique, each corrupted MB pixel is estimated with interpolation utilizing the nearest four adjoining MB pixels over the MB outlines. So, this technique is not appropriate with the restoration of texture characteristics, particularly in the case of heavily-erroneous channels, where almost all adjacent data has been lost or corrupted. The DIEC technique reconstructs the corrupted frame pixels by searching within the relative MBs to determine the object boundary orientation. The highest estimated value of the object boundary direction is chosen to recover the lost frames as noticed in Fig. 2d.

3. Suggested hybrid error recovery techniques

In this section, the proposed error recovery techniques for reconstructing the corrupted 3DV color and depth frames at the decoder side are introduced. The schematic framework of the proposed 3DV system with the enhanced proposed hybrid color-plus-depth EC techniques is presented in Fig. 3.

3.1. Suggested hybrid concealment techniques for the erroneous color frames

The suggested concealment techniques (CSOI, PMC, DTMC, and DIEC) for estimating the MVs and DVs of the erroneous color intra- and inter-frames are explained in this section. A full schematic diagram of the suggested combined color inter- and intra-frame EC techniques is introduced in Fig. 4. A hybrid method comprising spatial and temporal EC (CSOI + PMC) techniques is introduced for color intra-frames concealment, while a hybrid method comprising inter-view and temporal EC (DTMC + DIEC) techniques is presented for color inter-frames concealment.

The spatial WPAI technique cannot work efficiently in the case of heavy-loss channels, especially when a lot of surrounding MBs have been lost. In this paper, we propose a hybrid approach

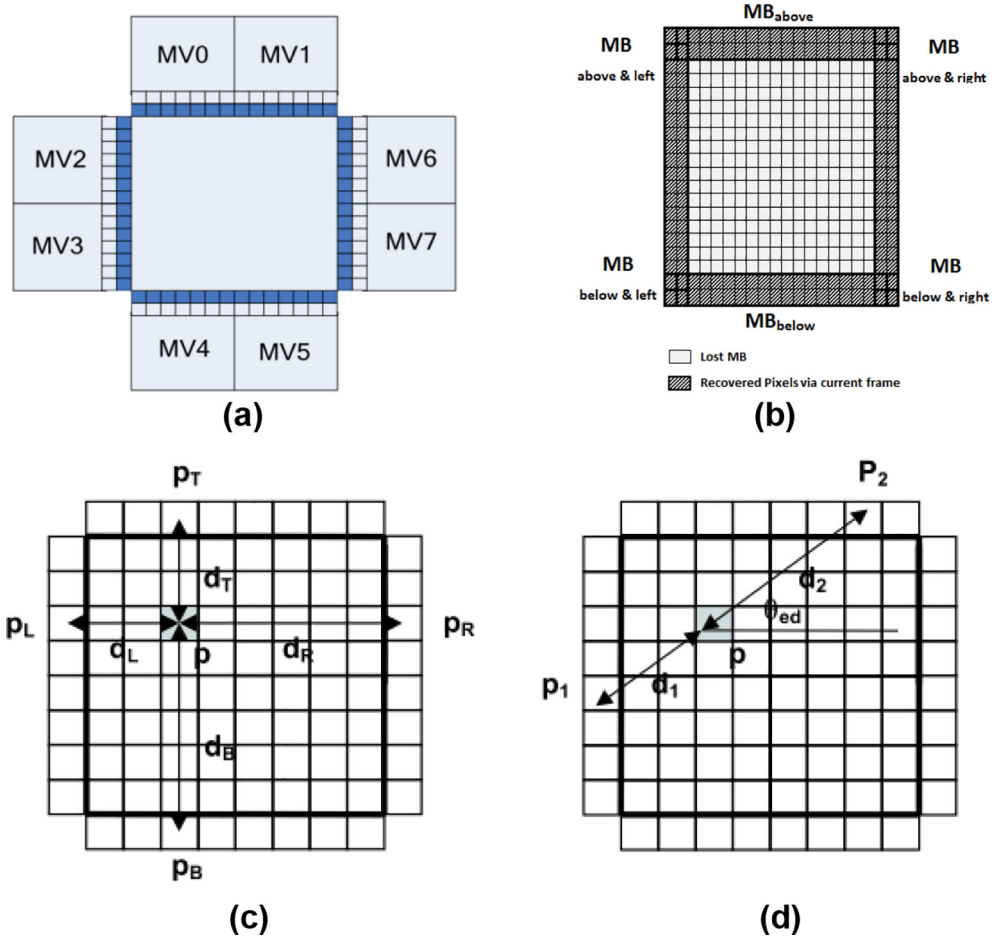

Fig. 2. The basic error recovery techniques. (a) OBBM, (b) DMVE, (c) WPAI, and (d) DIEC.

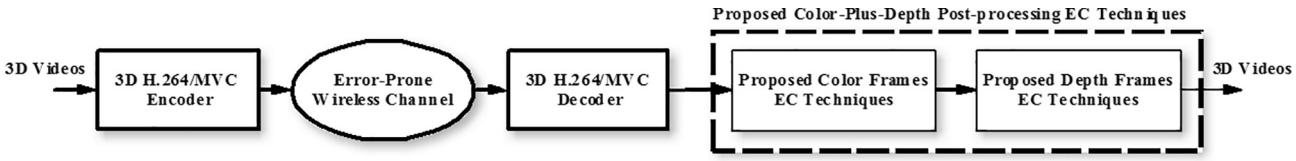

Fig. 3. General framework of the proposed 3DV color-plus-depth transmission system.

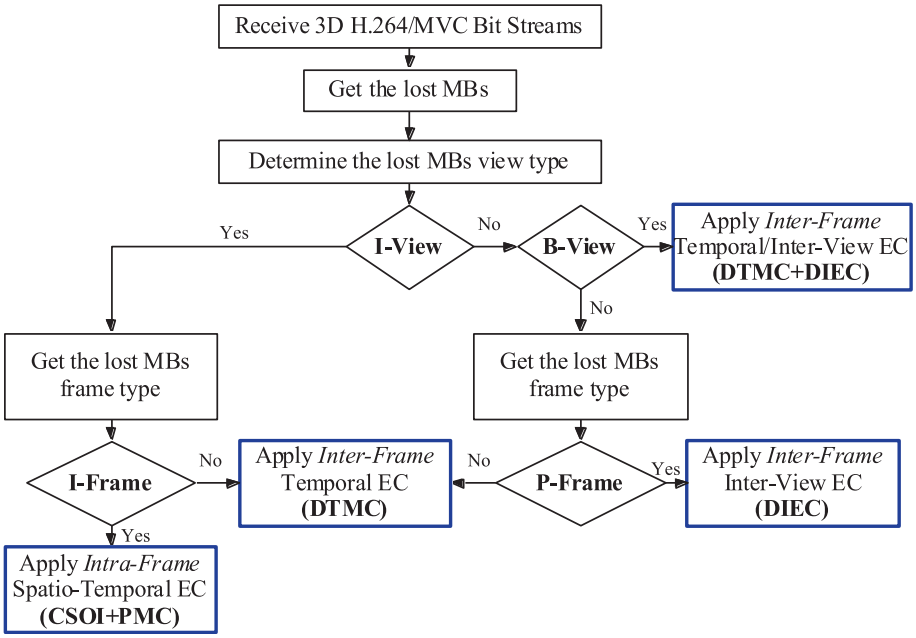

Fig. 4. The proposed framework of the hybrid EC techniques for the lost 3DV color frames.

comprising effective temporal PMC and spatial CSOI techniques for concealing the lost intra-frame MBs for achieving adequate intra-frames EC performance. The spatial interpolation CSOI technique works on a 4 × 4 MB to achieve a reliable EC performance. In the CSOI, the decoder can precisely determine the texture trend of the corrupted MB pixels and obtain the best interpolation along this direction. For each received corrupted 16 × 16 MB that has the same predicted direction, we divide it into sixteen 4 × 4 MBs that have different predicted directions. Then, the predicted direction of the correctly-received MBs is used to determine the best direction of the corrupted MB and estimate the lost MB pixels along the predicted direction. Thus, we calculate the superior estimated direction for the whole lost 4 × 4 MB pixels to improve the spatial EC performance. The spatial WPAI technique utilizes raster scanning to portend the 4 × 4 sixteen MBs from the left side to the right side, and thereafter from the upper to lower directions. So, this may introduce accumulation of errors with scanning (Yan and Zhou, 2012). Thence, the estimation errors will propagate to the reconstructed pixel values that will be used to restore the other erroneous pixels. Thus, the upper-left 4 × 4 MB has the smallest estimation accumulation error, whilst the lower-right 4 × 4 MB has the highest prediction accumulation error. To minimize the prediction error spreading and accumulation, a circular scanning order is proposed rather than the raster scanning order to determine the 4 × 4 sixteen MBs, and thus the spatial correlation among all 4 × 4 MBs is exploited, efficiently. Through the CSOI, firstly, we interpolate for the twelve 4 × 4 MBs at the edge, and then follow with the internal four 4 × 4 MBs as shown in Fig. 5. The MB number 1 has the smallest estimation error and the MB number 16 has the highest estimation error, because the prediction accumulation

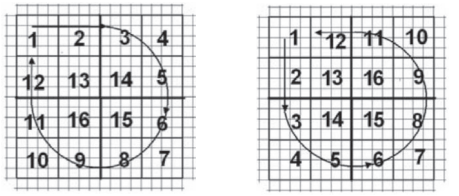

(a) Forward interpolation. **(b)** Backward interpolation.

Fig. 5. The proposed spatial CSOI technique.

error increases in the direction form MB 1 to MB 16. In order to avoid this scenario, both forward and backward circular interpolation directions are utilized as shown in Fig. 5, and the average of both interpolation cases is employed for the spatial concealment of the intra-frame errors.

To better enhance the subjective and objective 3DV qualities of the concealed intra-frames, the temporal PMC technique is jointly employed with the spatial CSOI technique. The PMC efficiently estimates the MVs of the lost MBs from the MVs of the correct adjacent MBs. Since the temporal OBBM technique recovers only one MV for the corrupted MB, this means that all pixels in the damaged MB will have the same MV intensity direction, which will result in decreasing the reconstruction quality, because only one MV cannot provide adequate reliability to conceal the heavy channel errors as the MB may include many direction details. Therefore, in this paper, the temporal PMC technique is exploited to enhance the MVs compensation for efficiently concealing the intra-frame errors. In the PMC, the corrupted MB is divided into four 8 × 8 blocks as shown in Fig. 6, so that there are four MVs needed for

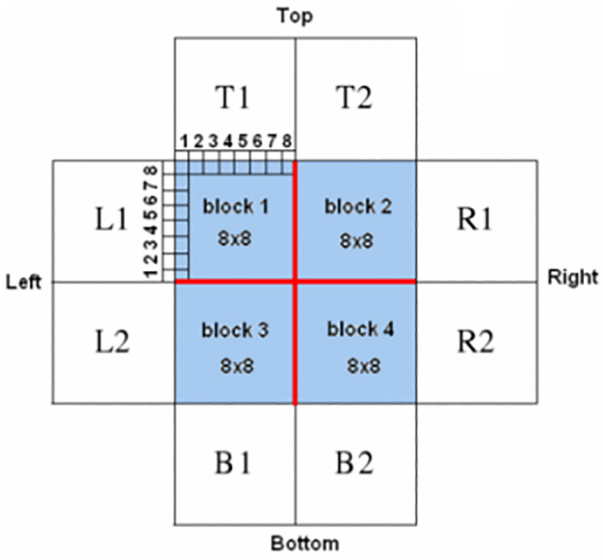

Fig. 6. The proposed temporal PMC technique.

estimating the damaged MB. Through the PMC, firstly the eight MVs for the eight 8×8 MBs (T1, T2, R1, R2, B1, B2, L1, L2) surrounding the lost MB are estimated, where the T, R, B, and L refer to the top, right, bottom, and left blocks. The MV_{L1} and MV_{T1} are used to estimate the MV_{Block1}. The MV_{T2} and MV_{R1} are exploited to evaluate the MV_{Block2}. The MV_{B1} and MV_{L2} are employed to calculate the MV_{Block3}. The MV_{R2} and the MV_{B2} are utilized to recover the MV_{Block4}. The MV_{Block1} is calculated by (1), where the $MV_{L1}(x, y)$ and the $MV_{T1}(x, y)$ are the estimated MVs values of block L1 and block T1, respectively. By the way, the MV_{Block2}, MV_{Block3}, and MV_{Block4} are calculated by (2)–(4), respectively. For each 8×8 block, there are 16 pixels on the border of each block as illustrated in Fig. 6. The Boundary Matching Error (BME) is estimated amongst the outside and inside MB boundary pixels with formula (5), where the $P_{inside}(j)$ is the pixel rate inside the MB boundary and the $P_{outside}(j)$ is the pixel rate of the neighboring blocks. So, the smallest BME of the candidate MVs within each block range will be selected as the optimum MV of the lost 8×8 block. So, there are four candidate concealment MVs rather than one candidate MV for concealing the damaged MB.

$$MV_{Block1}(x,y) : [\mathrm{Min}(MV_{L1}(x,y), MV_{T1}(x,y)), Max(MV_{L1}(x,y), MV_{T1}(x,y))] \quad (1)$$

$$MV_{Block2}(x,y) : [\mathrm{Min}(MV_{T2}(x,y), MV_{R1}(x,y)), Max(MV_{T2}(x,y), MV_{R1}(x,y))] \quad (2)$$

$$MV_{Block3}(x,y) : [\mathrm{Min}(MV_{L2}(x,y), MV_{B1}(x,y)), Max(MV_{L2}(x,y), MV_{B1}(x,y))] \quad (3)$$

$$MV_{Block4}(x,y) : [\mathrm{Min}(MV_{B2}(x,y), MV_{R2}(x,y)), Max(MV_{B2}(x,y), MV_{R2}(x,y))] \quad (4)$$

$$\mathrm{BME} = \left(\sum_{j=1}^{16} |(P_{inside}(j) - P_{outside}(j))| \right) / 16 \quad (5)$$

For the concealment of 3DV inter-frames, a hybrid approach comprising the efficient temporal DTMC and the inter-view DIEC techniques is proposed to reconstruct the MVs and DVs of the lost MBs. Unlike the OBBM technique that estimates one MV for the lost MB, the DTMC technique divides the MV space of the lost MB into eight different directional textural regions (R, T, L, B, TR, BR, TL, BL) as illustrated in Fig. 7, where the R, B, T, L, BR, TL, TR, and BL denote the right, bottom, top, left, bottom-right, top-left, top-right, and bottom-left surrounding MBs, respectively. The DTMC firstly checks the direction of the corrupted MB and its adjacent MBs with the co-located MBs in the reference frame. Then, it calculates eight directional candidate MVs among the damaged MB and its reference MB that has the same position and moving textural direction as the faulty MB in the reference related frame. So, the estimated eight different candidate MVs groups are given as Group T: {MV_{ref}, MV_T, MV_0}, Group B: {MV_{ref}, MV_B, MV_0}, Group R: {MV_{ref}, MV_R, MV_0}, Group L: {MV_{ref}, MV_L, MV_0}, Group TR: {MV_{ref}, MV_{TR}, MV_T, MV_R, MV_0}, Group TL: {MV_{ref}, MV_{TL}, MV_T, MV_L, MV_0}, Group BR: {MV_{ref}, MV_{BR}, MV_B, MV_R, MV_0}, Group BL: {MV_{ref}, MV_{BL}, MV_B, MV_L, MV_0}, and Group O: {MV_{ref}, MV_T, MV_{TR}, MV_R, MV_{BR}, MV_B, MV_{BL}, MV_L, MV_{TL}, MV_0, MV_{avg}}.

$$MV_{avg} = (MV_T + MV_B + MV_R + MV_L)/4 \quad (6)$$

where the MV_{avg} given in (6), and the MV_0 refer to the average MV and zero MV, respectively, and they are defined for the MBs in the slow-moving objects and background MBs. The group O is used, when the lost MB or its reference MB is found on the edge of the moving object. The DTMC selects the suitable group pf candidate MVs from the above-mentioned eight estimated groups depending on both textural directions of the adjoining MBs of the corrupted MB and the reference MB. So, for example, if the directions of both the MV_{ref} and MV_T are assigned in the T region, the group T is chosen for concealment, and so on.

To further improve the concealment efficiency of the erroneous MBs in the inter P and B frames, the DIEC is used as an inter-view EC technique to estimate the DVs. The DIEC recovers the corrupted MBs through investigating the contiguous frames to predict the object boundary outlines. The highest value of the object boundary direction is chosen to recover the lost frames as noticed in Fig. 2.d. It is used to calculate the DVs of the lost MBs in P frames in even V2, V4, and V6 views using its reference left inter-view frames. Also, it is employed to recover the corrupted MBs of B frames in odd V1, V3, and V5 views by determining the DVs of the corrupted MBs from their right and left relative frames in the neighboring views.

3.2. Suggested Depth-Assisted technique for the erroneous depth frames

In this section, the proposed depth-assisted error recovery technique for recovering the depth 3D video inter-frames and intra-frames is introduced. The suggested depth-assisted technique firstly calculates the MVs and DVs depth maps of the correctly and corruptly received bit streams. Since the DVs and MVs are estimated at the encoder side and transmitted to the decoder side, we can utilize them at the decoder side to estimate the depth data of the arriving MBs. The depth data maps of the properly-received

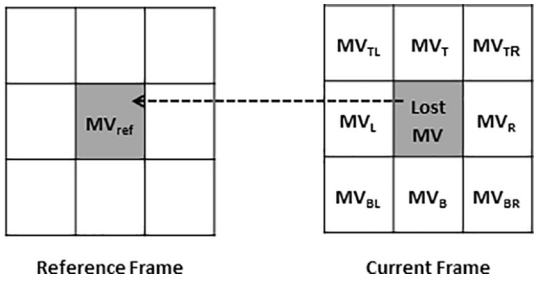

Fig. 7. The proposed temporal DTMC technique.

MBs in their relative MBs depending on the properly-received MVs and DVs, respectively, are found by (7) and (8).

$$d_{MV}(m,n) = k \times \sqrt{MV(m,n)_x^2 + MV(m,n)_y^2} \tag{7}$$

$$d_{DV}(m,n) = k \times \sqrt{DV(m,n)_x^2 + DV(m,n)_y^2} \tag{8}$$

where the $DV(m, n)$ and $MV(m, n)$ are the disparity and motion vectors at (m, n), k is a scaling factor, and the notations y and x represent the vertical and horizontal components of the MBs. Then, we calculate the inter-view and spatial–temporal (DVs and MVs) depth map values of the corrupted MBs in their relative adjacent frames by (9) and (10).

$$D_{MV}(m,n) = k \times \sqrt{\frac{MV_{F-1}(m,n)_x^2 + MV_{F-1}(m,n)_y^2 + MV_{F+1}(m,n)_x^2 + MV_{F+1}(m,n)_y^2}{2}} \tag{9}$$

$$D_{DV}(m,n) = k \times \sqrt{\frac{DV_{S-1}(m,n)_x^2 + DV_{S-1}(m,n)_y^2 + DV_{S+1}(m,n)_x^2 + DV_{S+1}(m,n)_y^2}{2}} \tag{10}$$

where S−1, S+1, F−1, and F+1 indicate the down, up, left, and right relative frames to the erroneous frame. After the estimation of disparity and motion depth data values for the frames with lost MBs in their reference collocated neighboring frames, the MCP and DCP are applied on the formerly-calculated depth data maps that are estimated by (9) and (10) to calculate the depth data of motion and disparity vectors. To collect the candidate depth MVs and DVs, the Sum of Absolute Difference (SAD) (El Shafai, 2011) is utilized as the calculation measure as indicated in (11)–(14).

$$SAD_{MV}(m,n) = \sum_{i=-R}^{R-1}\sum_{j=-R}^{R-1} |D_F(m,n) - D_{F-1}(m+i,n+j)| \tag{11}$$

$$SAD_{MV}(m,n) = \sum_{i=-R}^{R-1}\sum_{j=-R}^{R-1} |D_F(m,n) - D_{F+1}(m+i,n+j)| \tag{12}$$

$$SAD_{DV}(m,n) = \sum_{i=-R}^{R-1}\sum_{j=-R}^{R-1} |D_F(m,n) - D_{S-1}(m+i,n+j)| \tag{13}$$

$$SAD_{DV}(m,n) = \sum_{i=-R}^{R-1}\sum_{j=-R}^{R-1} |D_F(m,n) - D_{S+1}(m+i,n+j)| \tag{14}$$

where R is the search area, and $D_i(m, n)$ refers to the magnitude of the depth data at (m, n) of frame i. We assume that the MBs data inside the frame F are lost in the above formulas. Thus, the $D_F(m, n)$ is estimated by (9) or (10). The $D_{F-1}(m, n)$ and $D_{F+1}(m, n)$ are estimated by (7). Similarity, the $D_{S-1}(m, n)$ and $D_{S+1}(m, n)$ are estimated by (8). After the estimation of the reconstructed candidate depth motion and disparity vectors of the erroneously-received frames, we utilize the properly- and erroneously-received frames as explained formerly. Therefore, to enhance the EC efficiency, we as well collect the candidate group of color DVs and MVs for the corrupted frames in their relative frames. The color DVs and MVs are those related with the current lost MBs and the reference collocated MBs of their relative frames. They can be calculated with the in-detail EC procedures presented in Section 3.1. As explained formerly, the depth motion and disparity vectors of the erroneous MBs are estimated from the depth data maps with the same positions as the color motion and disparity vectors, whose depth data are calculated by (9) and (10). As well, we collect the depth motion and disparity vectors related with the correctly-received MBs, whose depth data values are calculated by (7) and (8). At this step, there are several estimated color-aided DVs and MVs concealment candidates besides the calculated depth-aided DVs and MVs concealment candidates. Thus, the DIEC and DMVE techniques are applied to choose the best concealment DVs and MVs from the complete obtained candidate group of color-aided and depth-aided DVs and MVs for restoring the corrupted color and depth MBs values of the received 3D video sequences, efficiently.

4. Experimental results and discussion

4.1. Performance assessment

In order to appraise the efficiency of the proposed hybrid color-plus-depth EC techniques, we have carried out different simulation experiments on well-known 3D video (Kendo, Balloons, and Ballet) sequences (mvc, 2016). The three tested 3D video streams have various features. The Kendo is an intermediate-moving stream, the Balloons is a moderate slow-moving stream, and the Ballet is a fast-moving stream. For each 3D video, the compressed 3D video bit streams are obtained, and then they are transmitted over a wireless network with various Packet Loss Rate (PLR) values. The received 3DV bit streams are decoded and recovered after that using the suggested EC techniques at the decoder side. In our simulation work, the JMVC reference software (Karunakar, 2014) is utilized based on the H.264 2D video reference codec (H.264/AVC, 2016). The simulation conditions used in this paper are chosen based on the JVT standard conditions (mvc, 2016). To assess the efficiency of the suggested EC techniques, the objective Peak Signal-to-Noise Ratio (PSNR) is used to determine the quality of the reconstructed and concealed 3DV frames.

To illustrate the effect of applying the proposed EC techniques for concealing the lost color-plus-depth 3DV frames through severely-corrupted channels, we have made some comparisons. We compared their efficiency performance to the state of employing the conventional state-of-the-art (WPAI and OBBM) color EC techniques without applying the proposed depth-assisted scheme (Conventional color-aided EC + No depth-aided EC) (El-Shafai, 2015), the case of utilizing the proposed (CSOI, PMC, DTMC, and DIEC) color EC techniques but without using the suggested depth-assisted scheme (Proposed color-aided EC + No depth-aided EC), and the state of no concealment (No color-aided concealment + No depth-aided concealment). In the presented experimental results, the proposed color-aided concealment + proposed depth-aided concealment gives the most reliable quality outcomes. The comparison of color and depth simulation results at various Quantization Parameters (QPs) of 37, 32, and 27, and at different severe PLRs of 30%, 40%, and 50% of the selected color and depth intra- and inter-frames of the chosen tested 3D video (Ballet, Kendo, and Balloons) streams are introduced in Figs. 8–10. For the 3DV tested sequences, different corrupted frame types and locations (P or B or I-frame) have been chosen within different-view positions to clarify the efficacy of the proposed EC techniques in concealing the corrupted frames inside any frame type or within any view location for different 3DV characteristics at different PLRs.

Fig. 8 introduces the color and depth frame subjective simulation results of the 3D video Ballet stream over a wireless channel with QP = 37 and PLR = 30% for the selected 17th intra-compressed color and depth I-frame within the I view V0. We reconstructed the simulated tested 17th color and depth frame based on the lossy indexed MB location in the lost view and frame using state-of-the-art EC methods without depth-aided EC as

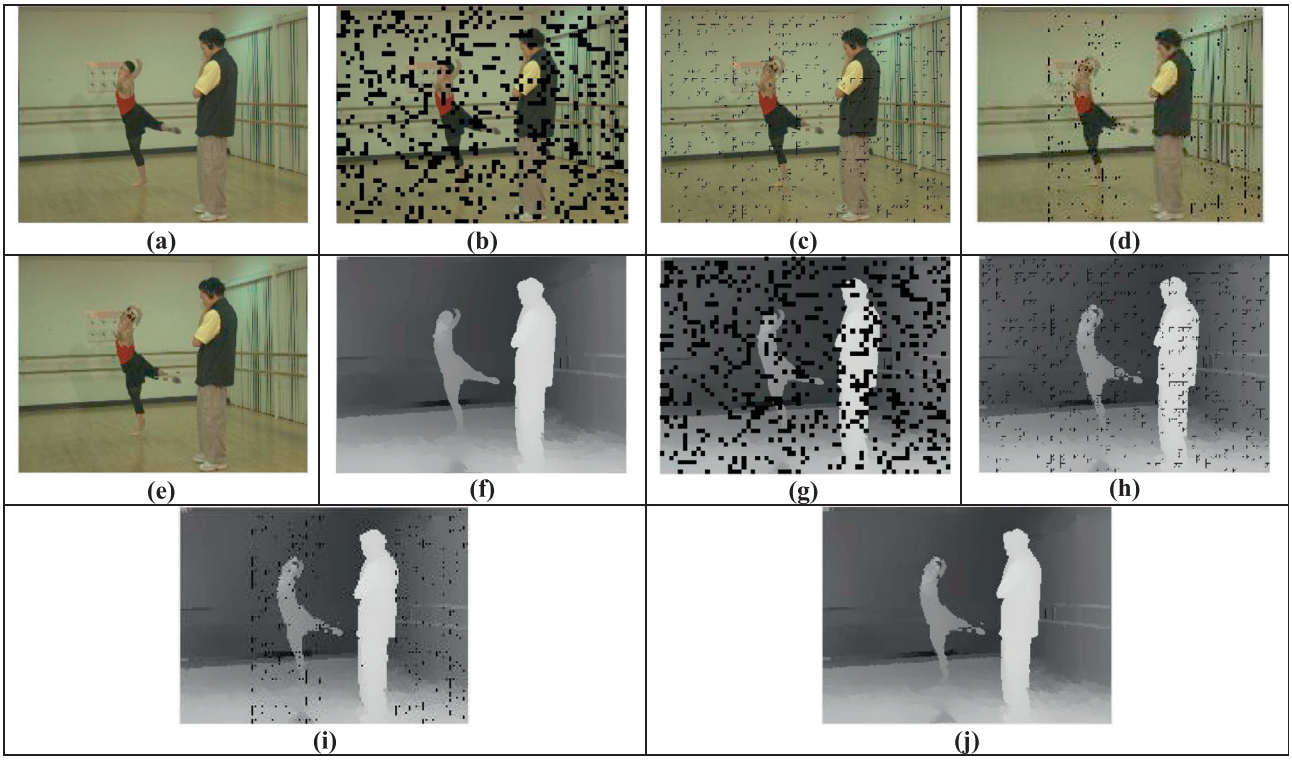

Fig. 8. Simulation results of the selected color and depth 17th I Intra-frame in the I view (V0) of the "Ballet" sequence: (a) Original error-free I_{17} color frame, (b) Corrupted I_{17} color frame with PLR = 30%, QP = 37, (c) Recovered I_{17} color frame with the case of conventional color-assisted EC + no depth-assisted EC (El-Shafai, 2015), (d) Concealed I_{17} color frame with the case of proposed color-assisted EC + no depth-assisted EC, (e) Concealed I_{17} color frame with the case of proposed color-assisted EC + proposed depth-assisted EC, (f) Original error-free I_{17} depth frame, (g) Corrupted I_{17} depth frame with PLR = 30%, QP = 37, (h) Recovered I_{17} depth frame with the case of conventional depth-assisted EC + no color-assisted EC (El-Shafai, 2015), (i) Concealed I_{17} depth frame with the proposed depth-assisted EC + no color-assisted EC, and (j) Concealed I_{17} depth frame with the case of proposed depth-assisted EC + proposed color-assisted EC.

introduced in Fig. 8c and h using the suggested EC techniques without exploiting the depth-assisted EC as shown in Fig. 8d and i, and finally using the full proposed hybrid color and depth EC techniques as given in Fig. 8e, and j. It is observed that the subjective results which are given in Fig. 8e and j of the color and depth frames for the suggested color-aided EC + proposed depth-aided EC techniques are better than those of the conventional color-aided EC + no depth-aided EC techniques (El-Shafai, 2015), and also those of the proposed color-aided EC + no depth-aided EC techniques as indicated in Fig. 8c and h, and Fig. 8d and i.

Fig. 9 shows the color and depth frames subjective simulation results of the 3D video Kendo stream over a wireless channel with QP = 32 and PLR = 40%. We have selected the 5th inter-compressed frame to test color and depth B frames inside the V1 B-view. From the presented recovered color and depth frames results in Fig. 9e, and j compared to those presented in Fig. 9c, d, h, and i, we notice that the full proposed hybrid color and depth EC techniques achieve good results in contrast to other error control techniques for recovering the corrupted color and depth frames efficiently in the state of severely-corrupted channels as in the state of PLR = 40%.

Fig. 10 presents the color and depth frames subjective simulation results of the 3D video Balloons stream over a wireless channel with QP = 27 and PLR = 50% for the simulated tested 73rd compressed color and depth P-frames inside the P-view V2. We notice from the obtained results in Fig. 10 that the subjective simulation results of the hybrid suggested color-aided concealment + depth-aided concealment schemes outperform those of the conventional color-aided concealment + no depth-aided concealment (El-Shafai, 2015) and the proposed color-aided concealment + no depth-aided concealment techniques. Therefore, the application of the joint suggested color and depth error control techniques is appreciated for recovering the corrupted color-plus-depth frames efficiently, particularly in the state of severely-corrupted wireless channels such as the state with PLR = 50%.

The comparisons of the PSNR simulation values of the simulated 3D video streams at various QPs and PLRs of 27, 32, and 37 are shown in Fig. 11, Table 1, and Fig. 12. We compared the PSNR simulation results of the proposed color and depth error control techniques (proposed color-aided EC + depth-aided EC) through the cases of using the literature state-of-the-art color EC methods without the proposed depth-assisted EC technique (conventional color-aided EC + no depth-aided EC) (El-Shafai, 2015), the proposed color EC techniques without the proposed depth-assisted EC technique (proposed color-aided EC + no depth-aided EC), and the case of no error control schemes (no color-aided concealment + no depth-aided concealment). As noticed from all the simulated 3D video streams, we perceive that the suggested color-based EC + depth-based EC techniques always achieve superior PSNR values. It can be observed that the suggested adaptive techniques have better average objective PSNR gain for the whole tested 3D video streams of about 1.23–2.05 dB, and 2.35–3.85 dB at various PLRs and QPs compared to the state of employing the proposed color-aided concealment + no depth-aided concealment technique, and the state of utilizing the conventional color-aided concealment + no depth-aided concealment technique (El-Shafai, 2015). We can also conclude that the proposed color-aided EC + depth-aided EC techniques are recommended as they provide about 11.28–24.35 dB objective PSNR values at various PLRs and QPs in contrast to the state of no EC techniques.

Also, we observed from all the simulation results that exploiting the suggested color and depth EC techniques is highly attractive in

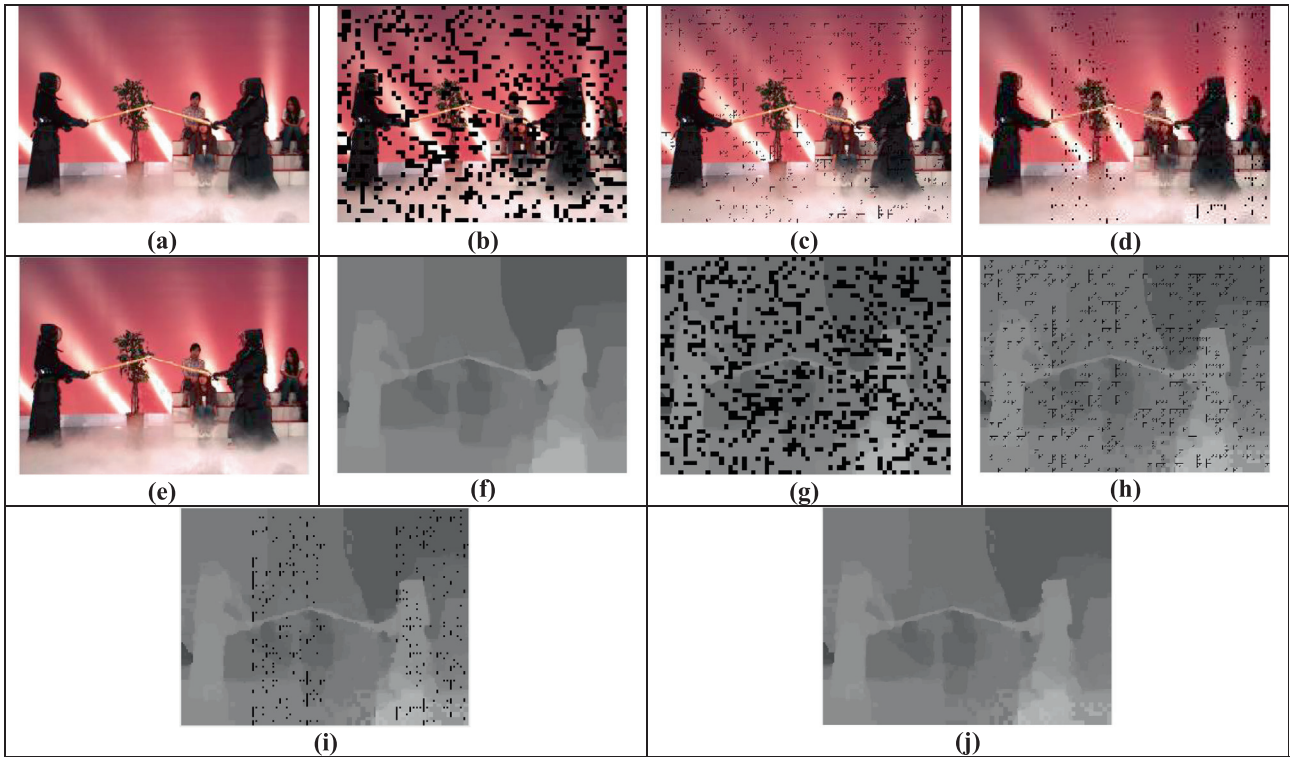

Fig. 9. Simulation results of the selected color and depth 5th B inter-frame in the B view (V1) of the "Kendo" sequence: (a) Original error-free B_5 color frame, (b) Corrupted B_5 color frame with PLR = 40%, QP = 32, (c) Recovered B_5 color frame with the case of conventional color-assisted EC + no depth-assisted EC (El-Shafai, 2015), (d) Concealed B_5 color frame with the proposed color-assisted EC + no depth-assisted EC, (e) Concealed B_5 color frame with the proposed color-assisted EC + proposed depth-assisted EC, (f) Original error-free B_5 depth frame, (g) Corrupted B_5 depth frame with PLR = 40%, QP = 32, (h) Recovered B_5 depth frame with the case of conventional depth-assisted EC + no color-assisted EC (El-Shafai, 2015), (i) Concealed B_5 depth frame with the proposed depth-assisted EC + no color-assisted EC, and (j) Concealed B_5 depth frame with the proposed depth-assisted EC + proposed color-assisted EC.

the state of severely-corrupted wireless channels. They have appreciated results compared to the state-of-the-art error control techniques. The simulation results clarify that there is a PSNR improvement obtained by the suggested techniques over those obtained by the other traditional techniques, and it becomes considerable whilst raising the PLRs or QPs. Moreover, it is observed that the proposed techniques introduce more efficient simulation results for 3D video sequences with various features, and they can conceal corrupted MBs within any view location with perfect efficacy.

4.2. Comparison study and discussions

To demonstrate and confirm the performance efficiency of the suggested concealment techniques for efficient 3DV communication through severe-packet-loss wireless channels, different experiments have been implemented with the JMVC software. The performances of the suggested techniques are compared with those of the FTR scheme, a hybrid technique of WPAI and OBBM (El Shafai, 2011), Hybrid Motion Vector Extrapolation (HMVE) (Lie et al., 2014), the Disparity Vector Extrapolation (DVE) (Hwang et al., 2008), hybrid DIEC and DMVE (El-Shafai, 2015), a joint technique of DMVE and DIEC methods applying the Flexible Macro-block Ordering (FMO) method (El-Shafai, 2015), and the four EC directional DV/MV determination techniques for a whole erroneous frame (Zhou et al., 2015). These traditional concealment schemes did not consider the depth-aided EC, but in the suggested techniques, we exploited both color and depth-aided recovery of DVs and MVs.

The comparison results are presented on the Balloons, Kendo, and Ballet well-known streams using the selfsame experimental conditions presented in Section 4.1 at different QPs and a PLR = 40%. All simulation experiments have been carried out utilizing Intel® Core™i7-4500U CPU @1.80 GHz and 2.40 GHz with 8 GB RAM and running with Windows 10 64-bit operating system. The objective PSNR and average frame execution time results are introduced to prove the efficiency of the proposed EC techniques. Table 2 presents the average PSNR values and frame execution time values of the suggested techniques compared to those of the FTR, HMVE, and DVE techniques, (Zhou et al., 2015; El Shafai, 2011; El-Shafai, 2015; El-Shafai, 2015) at different QPs of 27, 32, and 37. We notice that the suggested techniques outperform the traditional techniques in all experimental simulation configurations. It is also noticed that with the suggested reconstruction techniques, the 3DV quality can be further improved by taking advantage of the depth-aided EC in addition to the color-aided EC techniques. Furthermore, it is observed that the suggested techniques have slightly longer processing times compared to those of the traditional techniques. Therefore, the processing times of the suggested techniques may be suitable for real-time and online 3DV streaming implementations.

We verified the performance of the suggested EC techniques compared to the performance of the traditional state-of-the-art techniques exploiting the depth-aided concealment in (Yan and Zhou, 2012; Wang and Wang, 2016; Mueller and Vetro, 2014). Those traditional techniques make use of the advantage of depth-aided EC in addition to color-aided EC. However, they compress and extrapolate the depth data maps at the encoder side and transport them over the wireless network. Thus, they increase the calculation complexity and communication bit rate of the 3D video system. So, they may not be appropriate for the limited resources of wireless channels. The comparison experiments have been carried out on the tested 3D Balloons and Kendo streams at a communication PLR = 20% and QP = 27. Table 3 presents the average objective PSNR and frame execution times of the suggested

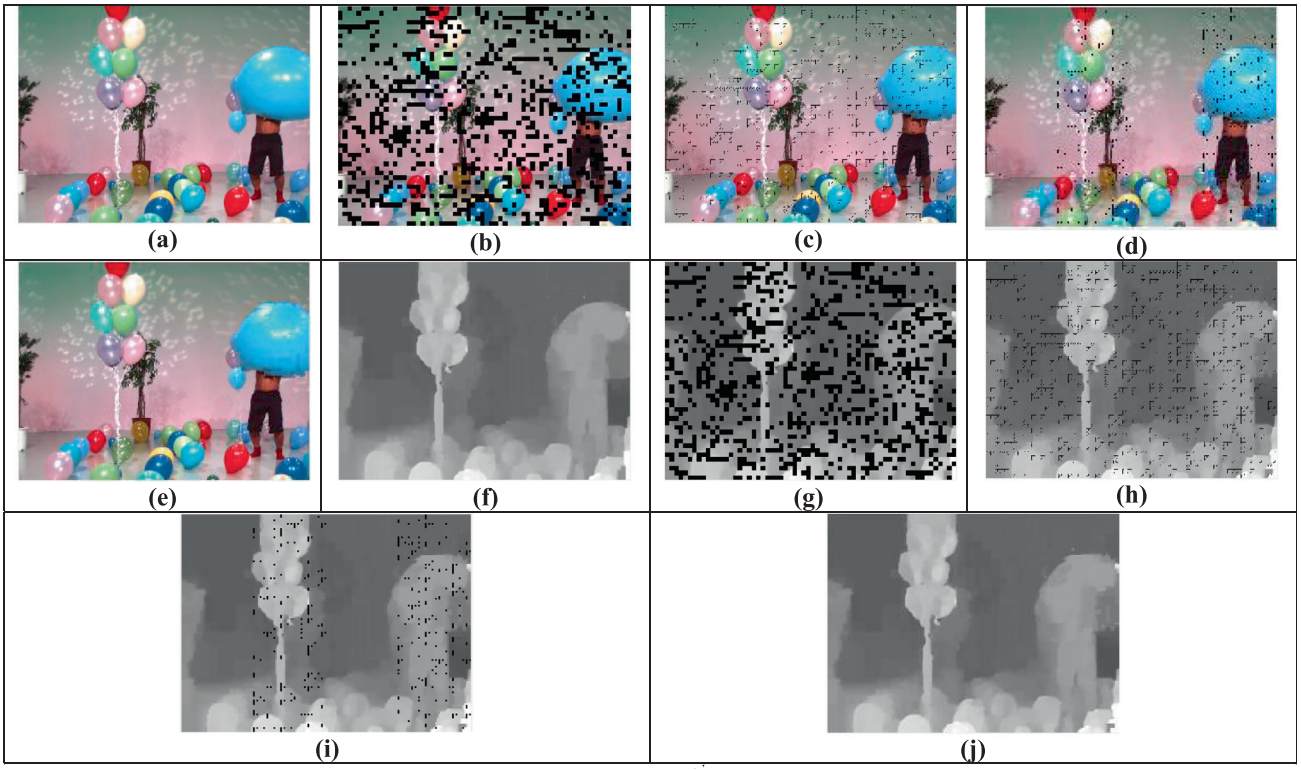

Fig. 10. Simulation results of the selected color and depth 73rd P inter-frame in the P view (V2) of the "Balloons" sequence: (a) Original error-free P_{73} color frame, (b) Corrupted P_{73} color frame with PLR = 50%, QP = 27, (c) Recovered P_{73} color frame with the case of conventional color-assisted EC + no depth-assisted EC (El-Shafai, 2015), (d) Concealed P_{73} color frame with the proposed color-assisted EC + no depth-assisted EC, (e) Concealed P_{73} color frame with the proposed color-assisted EC + proposed depth-assisted EC, (f) Original error-free P_{73} depth frame, (g) Corrupted P_{73} depth frame with PLR = 50%, QP = 27, (h) Recovered P_{73} depth frame with the case of conventional depth-assisted EC + no color-assisted EC (El-Shafai, 2015), (i) Concealed P_{73} depth frame with the proposed depth-assisted EC + no color-assisted EC, and (j) Concealed P_{73} depth frame with the proposed depth-assisted EC + proposed Color-assisted EC.

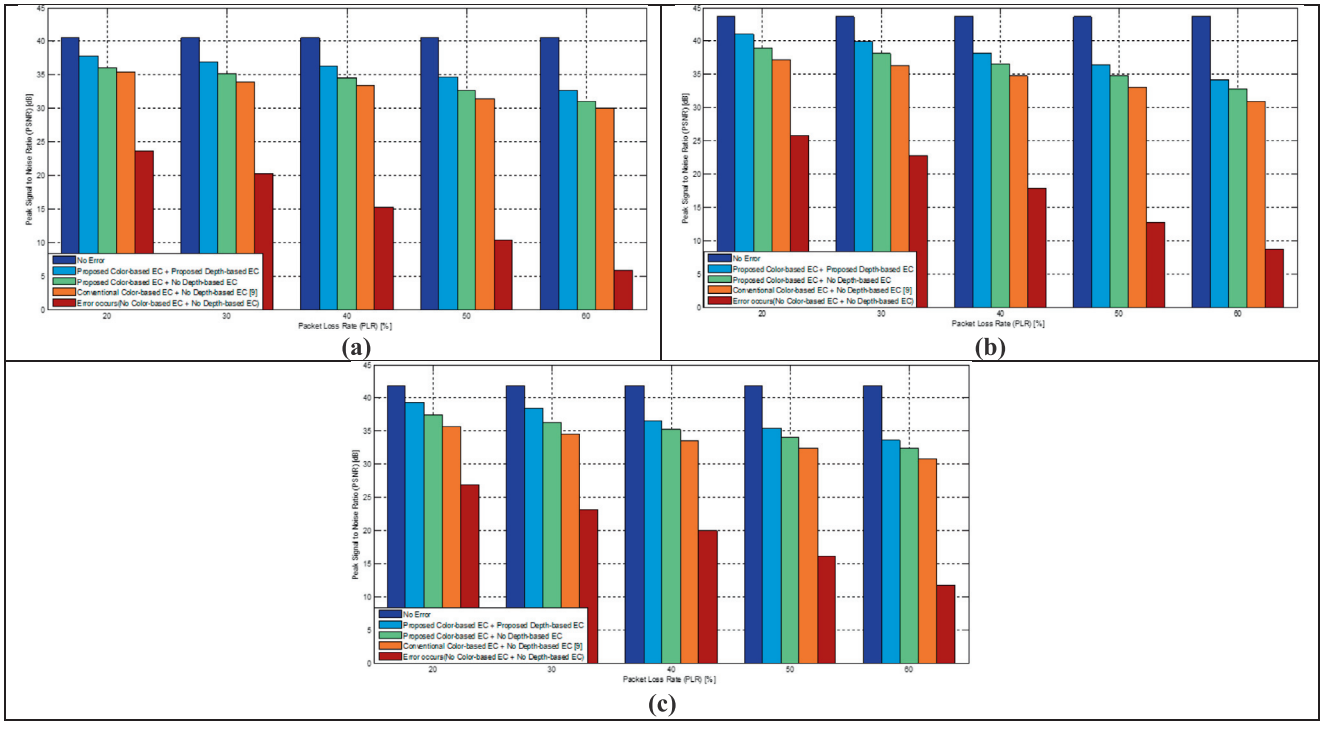

Fig. 11. Objective PSNR (dB) results of the tested: (a) Ballet, (b) Kendo, and (c) Balloons 3D video sequences at QP = 27 and various PLRs.

Table 1
Objective PSNR (dB) results of the tested: (a) Ballet, (b) Kendo, and (c) Balloons 3D video sequences at QP = 32 and various PLRs.

Sequence	Packet loss rate (PLR)%					
	Applied scheme	20%	30%	40%	50%	60%
Ballet	No Error	38.70	38.70	38.70	38.70	38.70
	Proposed color-based EC + Proposed depth-based EC	**35.52**	**33.86**	**32.97**	**31.46**	**29.53**
	Proposed color-based EC + No depth-based EC	32.57	32.09	31.17	29.69	27.87
	Conventional color-based EC + No depth-based EC (El-Shafai, 2015)	31.63	31.20	30.32	28.89	26.11
	Error occurs (No color-based EC + No depth-based EC)	21.59	18.84	14.56	9.97	5.71
Kendo	No Error	43.03	43.03	43.03	43.03	43.03
	Proposed color-based EC + Proposed depth-based EC	**38.78**	**37.81**	**36.22**	**34.39**	**32.43**
	Proposed color-based EC + no depth-based EC	37.05	36.10	34.61	32.83	30.94
	Conventional color-based EC + No depth-based EC (El-Shafai, 2015)	35.12	34.19	32.70	31.04	29.16
	Error occurs (No color-based EC + No depth-based EC)	24.38	21.19	16.91	12.33	8.18
Balloons	No Error	41.13	41.13	41.13	41.13	41.13
	Proposed color-based EC + Proposed depth-based EC	**37.86**	**36.05**	**34.62**	**33.37**	**31.41**
	Proposed color-based EC + No depth-based EC	35.32	34.25	32.92	31.67	29.75
	Conventional color-based EC + No depth-based EC (El-Shafai, 2015)	33.48	32.44	31.14	29.83	28.09
	Error occurs (No color-based EC + No depth-based EC)	25.92	22.23	19.06	15.43	11.48

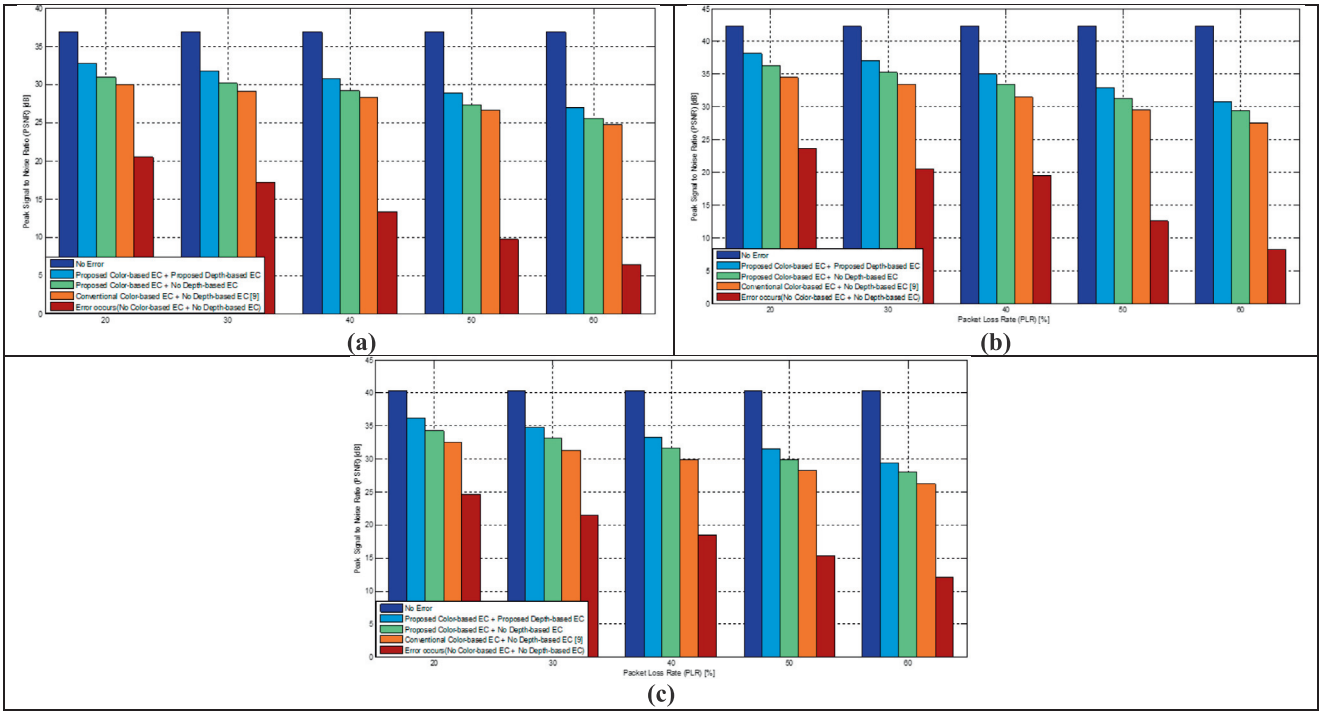

Fig. 12. Objective PSNR (dB) results of the tested: (a) Ballet, (b) Kendo, and (c) Balloons 3D video sequences at QP = 37 and various PLRs.

techniques compared to the traditional state-of-the-art color- and depth-aided EC methods in (Yan and Zhou, 2012; Wang and Wang, 2016; Mueller and Vetro, 2014). It is observed that the suggested techniques outperform these traditional techniques, and they achieve objective PSNR performance refinements by employing color-plus-depth EC schemes. Furthermore, the suggested techniques cause a minimal increment in the processing time compared to some of the traditional works, and thence they are acceptable and compatible with online 3D video communication. In addition, the suggested techniques have the merit of extracting the depth data maps at the decoder side instead of doing that at the encoder side, and so they work efficiently compared to the state-of-the-art methods.

In Karunakar (2014), an effort to improve the quality of rendered views obtained from 3DV decoded depth-maps was introduced. The authors proposed a post-processing technique that is based on compression artifact analysis of depth maps. They implemented a post-processing filter framework, which involves two-stage filtering; an edge-adaptive joint trilateral filter followed by histogram analysis and an adaptive bilateral filter. This technique studied only the effect of compression artifacts and ignored the effect of transmission artifacts. On the other hand, in our proposed work, we study the effect of both compression and transmission artifacts effects. We compared the proposed hybrid post-processing error recovery techniques in this paper with that presented in Karunakar (2014) to prove the efficiency of our proposed hybrid techniques. The comparison experiments have been carried out on the tested 3D Balloons and Kendo streams at QP = 27. Table 4 presents the average objective PSNR and the average Structural Similarity (SSIM) index of the suggested techniques compared to the traditional state-of-the-art work in Karunakar (2014). It is observed that the suggested techniques outperform the traditional technique in Karunakar (2014), and they achieve better objective PSNR and SSIM values.

Table 2
Objective average PSNR (dB) and execution times of the suggested techniques and the literature techniques on the 3DV tested Balloons, Kendo, and Ballet streams at different QPs and a PLR = 40%.

QP	Sequence	PSNR (dB)/execution time per frame (s)								
		Origin	FTR	DVE	HMVE	Zhou et al. (2015)	El Shafai (2011)	El-Shafai (2015)	El-Shafai, (2015)	**Proposed**
27	Ballet	40.58/0.039	32.53/0.041	26.67/0.043	32.68/0.043	33.67/0.048	34.43/0.042	35.85/0.052	37.38/0.059	**37.84/0.066**
	Kendo	43.72/0.050	25.58/0.052	24.82/0.055	26.18/0.054	28.37/0.058	37.47/0.056	38.62/0.064	39.95/0.071	**41.06/0.082**
	Balloons	41.92/0.043	32.80/0.045	31.27/0.046	35.64/0.048	36.33/0.054	36.81/0.059	37.69/0.067	38.95/0.074	**39.33/0.079**
32	Ballet	38.70/0.041	32.04/0.042	26.79/0.044	32.29/0.045	33.26/0.051	32.67/0.049	33.92/0.058	35.13/0.067	**35.52/0.073**
	Kendo	43.03/0.053	25.52/0.055	25.41/0.057	26.83/0.058	28.23/0.063	36.59/0.067	37.54/0.070	38.72/0.076	**38.78/0.089**
	Balloons	41.13/0.044	32.43/0.046	32.08/0.047	34.36/0.051	34.83/0.056	35.53/0.060	36.28/0.069	37.43/0.078	**37.86/0.083**
37	Ballet	36.84/0.043	31.49/0.047	27.10/0.049	31.83/0.052	32.61/0.056	30.73/0.061	31.62/0.069	32.62/0.077	**32.75/0.076**
	Kendo	42.29/0.055	25.40/0.058	25.69/0.061	26.87/0.063	27.92/0.067	35.61/0.065	36.46/0.073	37.35/0.080	**38.19/0.091**
	Balloons	40.41/0.047	32.15/0.050	32.17/0.052	32.92/0.051	33.29/0.056	34.73/0.055	35.49/0.064	36.48/0.074	**36.79/0.086**

Table 3
Objective average PSNR (dB) and execution times of the suggested techniques and the traditional color- and depth-aided EC techniques on the 3DV tested Balloons and Kendo streams at PLR = 20% and QP = 27.

Sequence	PSNR (dB)/Execution time per frame (s)				
	Origin	(Yan and Zhou, 2012)	(Wang and Wang, 2016)	(Mueller and Vetro, 2014)	**Proposed**
Kendo	43.72/0.050	28.87/0.063	39.38/0.079	37.51/0.082	**41.06/0.080**
Balloons	41.92/0.043	36.34/0.056	39.66/0.068	35.88/0.073	**39.33/0.071**

Table 4
Objective average PSNR (dB) and SSIM values of the suggested techniques and the traditional post-processing technique in (Karunakar, 2014) on the 3DV tested Balloons and Kendo streams at QP = 27.

Sequence	**PSNR (dB)/SSIM**	
	Karunakar (2014)	**Proposed**
Kendo	40.82/0.9466	**41.06/0.9508**
Balloons	38.26/0.9143	**39.33/0.9564**

5. Conclusions

This work suggested improved hybrid error recovery techniques at the decoder side for corrupted color-plus-depth MBs of the 3D-MVC transmitted through lossy wireless networks. The major significant strength of this paper is the employment of depth DVs and MVs without compressing and transporting depth data to avert complicated depth calculations at the encoder side. Furthermore, the suitable concealment technique is adaptively selected depending on the lost depth or color erroneous view and frame. Moreover, the suggested techniques confirmed that they are more reliable and desirable in the state of severe corrupted wireless channel conditions. Simulation results proved the accomplishments of the suggested techniques in recovering the transmitted severely-erroneous color-plus-depth 3D video streams with high PLRs. They achieved good subjective 3DV quality, and also favorable objective PSNRs with acceptable processing times.

References

Assunçao, P.A.A., Marcelino, S., Soares, S., de Faria, S.M., 2017. Spatial error concealment for intra-coded depth maps in multiview video-plus-depth. Multimedia Tool. Appl., 1–24

Chung, T.Y., Sull, S., Kim, C.S., 2011. Frame loss concealment for stereoscopic video plus depth sequences. IEEE Trans. Consum. Electron. 57 (3).

De Abreu, A., Frossard, P., Pereira, F., 2015. Optimizing multiview video plus depth prediction structures for interactive multiview video streaming. IEEE J. Selec. Top. Signal Process. 9 (3), 487–500.

El Shafai, W., Hrušovský, B., El-Khamy, M., El-Sharkawy, M. (2011, September). Joint space-time-view error concealment algorithms for 3D multi-view video. In: Image Processing (ICIP), 2011 18th IEEE International Conference on, pp. 2201–2204.

El-Shafai, W., 2015. Pixel-level matching based multi-hypothesis error concealment modes for wireless 3D H. 264/MVC communication. 3D Research 6 (3), 31.

El-Shafai, W., 2015. Joint adaptive pre-processing resilience and post-processing concealment schemes for 3D video transmission. 3D Research 6 (1), 1–13.

El-Shafai, W., El-Rabaie, S., El-Halawany, M.M., El-Samie, F.E.A., 2017b. Encoder-independent decoder-dependent depth-assisted error concealment algorithm for wireless 3D video communication. Multimedia Tool. Appl., 1–28

El-Shafai, W., El-Rabaie, S., El-Halawany, M., El-Samie, F.A., 2017a. Enhancement of wireless 3d video communication using color-plus-depth error restoration algorithms and bayesian kalman filtering. Wireless Pers. Commun., 1–24

El-Shafai, W. (2013). Optimized Adaptive Space-Time-View Multi-Dimentional Error Concealment for 3D Multi-View Video transmission. In: Electronics, Communications and Photonics Conference (SIECPC), Saudi International, pp. 1–6. IEEE.

Gadgil, N., Li, H., Delp, E. J. (2015). Spatial subsampling-based multiple description video coding with adaptive temporal-spatial error concealment. In: Picture Coding Symposium (PCS), 2015, pp. 90–94. IEEE.

http://iphome.hhi.de/suehring/tml/: H.264/AVC codec, (accessed 20.09.2016.).

Hewage, C.T., Martini, M.G., 2013. Quality of experience for 3D video streaming. IEEE Commun. Magaz. 51 (5), 101–107.

Huo, Y., El-Hajjar, M., Hanzo, L., 2013. Inter-layer FEC aided unequal error protection for multilayer video transmission in mobile TV. IEEE Trans. Circuits Syst. Video Technol. 23 (9), 1622–1634.

Hwang, M.C., Kim, J.H., Duong, D.T., Ko, S.J., 2008. Hybrid temporal error concealment methods for block-based compressed video transmission. IEEE Trans. Broadcast. 54 (2), 198–207.

Karunakar, P.N. (2014). Implementation of an out-of-the loop post-processing technique for HEVC decoded depth maps. Master thesis.

Khattak, S., Maugey, T., Hamzaoui, R., Ahmad, S., Frossard, P., 2016. Temporal and inter-view consistent error concealment technique for multiview plus depth video. IEEE Trans. Circuits Syst. Video Technol. 26 (5), 829–840.

Lee, P.J., Kuo, K.T., Chi, C.Y., 2014. An adaptive error concealment method based on fuzzy reasoning for multi-view video coding. J. Display Technol. 10 (7), 560–567.

Lie, W. N., Lin, G. H. (2013). Error concealment for 3D video transmission. In: Circuits and Systems (ISCAS), 2013 IEEE International Symposium on. pp. 2856–2559.

Lie, W.N., Lee, C.M., Yeh, C.H., Gao, Z.W., 2014. Motion vector recovery for video error concealment by using iterative dynamic-programming optimization. IEEE Trans. Multimed. 16 (1), 216–227.

Liu, Z., Cheung, G., Ji, Y., 2013. Optimizing distributed source coding for interactive multiview video streaming over lossy networks. IEEE Trans. Circuits System. Video Technol. 23 (10), 1781–1794.

Mueller, K., Vetro, A. (2014) Common test conditions of 3D-MVV core experiments. Joint Collaborative Team on 3D Video Coding Extensions JCT3V-G1100, 7th Meeting: San Jose, USA.

http://wftp3.itu.int/av-arch/jvt-site/2009_01_Geneva/JVT-AD207.zip: Reference software for multiview video coding (mvc), (accessed 20.09.2016.).

Ozcinar, C., Ekmekcioglu, E., Ćalić, J., Kondoz, A., 2016. Adaptive delivery of immersive 3D multi-view video over the Internet. Multimedia Tool. Appl. 75 (20), 12431–12461.

Purica, A.I., Mora, E.G., Pesquet-Popescu, B., Cagnazzo, M., Ionescu, B., 2016. Multiview plus depth video coding with temporal prediction view synthesis. IEEE Trans. Circuits Syst. Video Technol. 26 (2), 360–374.

Salim, O. H., Xiang, W., Leis, J. (2013). An efficient unequal error protection scheme for 3-D video transmission. In Wireless Communications and Networking Conference (WCNC), 2013 IEEE. pp. 4077–4082.

Tai, S.C., Wang, C.C., Hong, C.S., Luo, Y.C., 2016. An effiicient full frame algorithm for object-based error concealment in 3D depth-based video. Multimedia Tool. Appl. 75 (16), 9927–9947.

Wang, H., Wang, X., 2016. Important macroblock distinction model for multi-view plus depth video transmission over error-prone network. Multimedia Tool. Appl., 1–23

Xiang, W., Gao, P., Peng, Q., 2015. Robust multiview three-dimensional video communications based on distributed video coding. IEEE Syst. J., 1–11

Yan, B., Zhou, J., 2012. Efficient frame concealment for depth image-based 3-D video transmission. IEEE Trans. Multimedia 14 (3), 936–941.

Zhou, Y., Xiang, W., Wang, G., 2015. Frame loss concealment for multiview video transmission over wireless multimedia sensor networks. IEEE Sens. J. 15 (3), 1892–1901.